HUMANOID HUMERAL POINTING KINEMATICS

Jadran Lenarčič
J Stefan Institute
University of Ljubljana, Slovenia
jadran.lenarcic@ijs.si

Michael Stanišić and Eric Schearer
University of Notre Dame
Notre Dame, IN. USA
stanisic@nd.edu

Abstract Humanoid humeral pointing kinematics is implemented in a humanoid robotic shoulder complex consisting of a parallel mechanism as the innermost shoulder girdle and a serial mechanism as the outermost spherical glenohumeral joint. These subsystems operate cooperatively as an offset double pointing system. The humanoid humeral pointing kinematics are also implemented within a passive humanoid shoulder complex.

Keywords: Humanoid Shoulder, Shoulder Girdle, Parallel Mechanism

1. Primary function of the human shoulder complex in human arm motions

The human shoulder complex is divided into two subsystems. The innermost portion, the *shoulder girdle*, consists of the sternum, thorax, torso, clavicle and scapula. The outermost portion, the *glenohumeral joint*, connects the humerus to the scapula Zatsiorsky, 1997. The primary function of the human shoulder complex is pointing the humerus. With a roll about the pointed humeral axis the elbow orientation is controlled. Human shoulder girdle motion is primarily a consequence of this humeral pointing.

In the human shoulder complex (Fig. 1) the girdle is a closed-loop chain, the glenohumeral joint is a serial chain. The girdle bears full load and inertial forces of the arm and manipulated object, while developing a small motion. Without this small motion the human's humeral workspace would be much less than a hemisphere.

On the right side of Fig. 1, the human shoulder girdle is overlayed by a simple kinematic equivalent, consisting of a universal joint centered at

J. Lenarčič and F. Thomas (eds.), Advances in Robot Kinematics, 79–88.

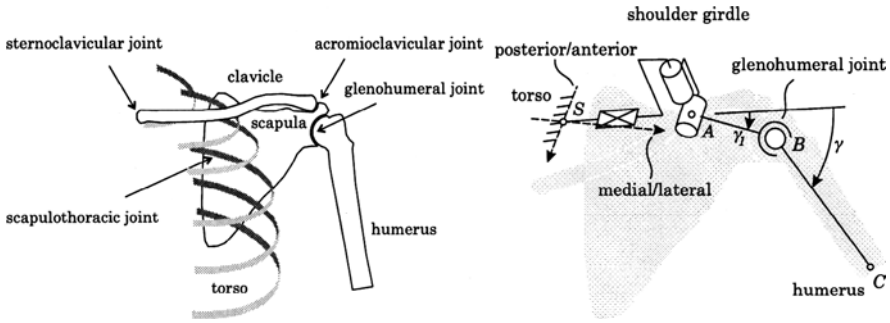

Figure 1. The human shoulder complex (frontal view) and a kinematic equivalent of the human shoulder complex.

point A. The center of the glenohumeral joint is point B. Point S represents a fixed reference placed at the intersection of the posterior/anterior axis passing through the center of the sternoclavicular joint and the medial/lateral axis through the middle of the torso. To mimic the distance between points S and B a translation is introduced, which is a dependent coordinate treated as a function of the rotation angles at A.

In Kohne et al., 2001, the relative position between points S and B was measured in humans performing different manipulation tasks. The maximum working cone of axis $\overline{SB}$ is produced when the humerus is stretched downward. An average maximum cone angle is about 50°. The central cone axis inclines 10° upward and 5° forward with respect to the medial/lateral axis. The distance between points S and B changes about ±10% of the average value as a function of the inclination angle between axis $\overline{SB}$ and the central axis of its working cone. $\overline{SB}$ shortens when the girdle moves upward and backward and lengthens when the girdle is moving downward and forward.

During humerus elevation the glenoid fossa (on which the humerus moves) tilts upward. This conjoint movement is the "shoulder rhythm" Dvir and Berme, 1978, illustrated in two images on the right side of Fig. 3. Measurement of the shoulder rhythm in the frontal plane Inman et al., 1944, Dvir and Berme, 1978, Umek-Venturini and Lenarčič, 1996, show that to a given angle γ corresponds an angle γ_1 (Fig. 3) which is associated with the lower reach of axis $\overline{AB}$. The upper reach is constant and is delimited by the working cone of this axis. Increase in the humeral elevation causes a decrease in the girdle's range, as well as in the kinematic redundancy of the shoulder complex. The ratio between γ_1 and γ is nearly constant for all γ and differs among subjects. In a first approximation, $\gamma_1 : \gamma = 1 : 3$.

The humerus and girdle move conjointly in the horizontal plane and any other plane intersecting axis $\overline{SA}$. *Humanoid pointing is defined as a configuration in which the displacement of the shoulder girdle and the humerus are co-planar and the relationship between angles γ_1 and γ achieves a value consistent with a measured human ratio.*

2. A humanoid shoulder complex

Fig. 2 shows a serial humanoid shoulder complex developing the shoulder girdle and glenohumeral joint movements shown in the kinematic model on the right side of Fig. 1. Point A in Fig. (2) is the center

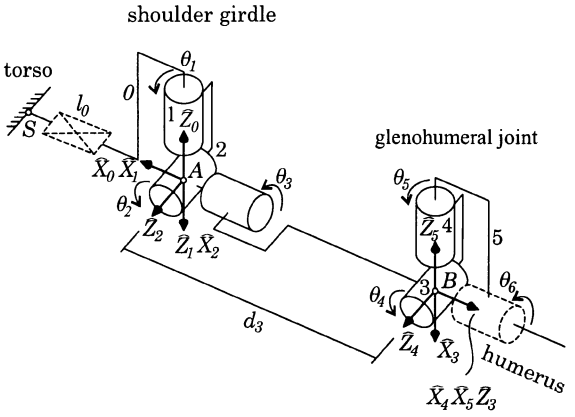

Figure 2. A serial humanoid shoulder complex.

for the non-synovial gliding motion of the scapula over the back of the thorax. Of three rotations associated with center A, θ_1 and θ_2 form the innermost pointing system. θ_3 is introduced to optimize performance of a parallel mechanism introduced later. Linear displacement l_0 develops the bulk of what is a moving center for the motion of the scapula over the thorax.

Point B in Fig. (2) is the center for pointing motion in the glenohumeral joint. This center is not fixed in the human but its movement is small and it is not necessary to cause it to displace. Two rotations, θ_4, θ_5 are necessary for pointing. θ_6, develops the humeral roll and does not contribute to humeral pointing.

The serial model in Fig. 2 incorporates a parallel mechanism shrouding center A which allows for controlling the three rotations at center A with leg lengths l_1, l_2 and l_3, shown on the left side of Fig. 3. The parallel mechanism increases load carrying capacity and rigidity of cen-

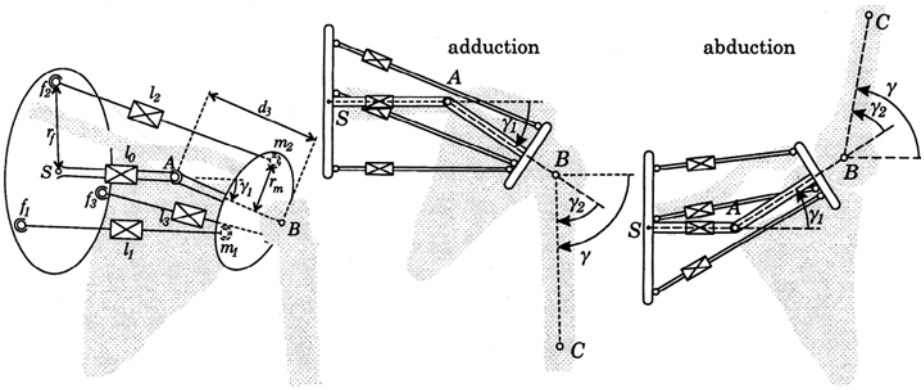

Figure 3. The parallel mechanism humanoid shoulder girdle and the complex in abduction-adduction.

ter A. Legs l_1, l_2 and l_3 represent the combined action of the human clavicle and ligaments which constrain the gliding of the human scapula over the thorax. The two images on the right side of Fig. 3 show the frontal view of the left arm in its minimum and maximum elevation, overlaid by the corresponding configurations of the humanoid shoulder complex. The lateral size of the humanoid shoulder girdle is represented by d_3, the distance between centers A and B in Fig. 2. The maximum inclination angle γ_1 at center A is 32° and the extension/contraction of the central leg varies within $l_0 = d_3 \pm 10\%$. Details on the design of this parallel mechanism are discussed in Lenarčič et al.(a), 2000, Lenarčič et al.(b), 2000.

This shoulder complex has seven degrees of freedom, four in the girdle (l_0,l_1,l_2,l_3) and three in the glenohumeral joint (θ_4,θ_5,θ_6). Neither l_0 or θ_6 contribute to humeral pointing and are not considered further. l_0 depends on γ_1 and θ_6 determines the final elbow orientation. Analogous to human humeral pointing, *humanoid humeral pointing occurs when line segments* $\overline{SA}$, $\overline{AB}$, *and* $\overline{BC}$ *are co-planar and the ratio between angles* γ_1 *and* γ_2 *achieves an anatomically consistent value.*

3. Humanoid humeral pointing kinematics of the serial shoulder complex

Values of γ_1 and γ_2 vary as functions of the pose of the girdle and have an anatomical background obtained by measuring a human performing the task of pointing. We incorporate this anatomical dependency within the humanoid shoulder complex.

Frame assignments, DH parameters and notation follow Craig, 1989. Table 1 gives the DH parameters for the serial chain in Fig. 2. The $\hat{X}_5$ axis is the axis of the humanoid humerus, pointing from center B to the elbow axis (which is not shown). This serial chain forms a double pointing system, with rotations θ_1, θ_2 and θ_3 at center A and rotations θ_4, θ_5 and θ_6 at center B. d_3 represents the lateral width of the humanoid shoulder girdle.

The forward humeral pointing kinematic equations are developed using the homogeneeous transformations ${}^{i-1}_{i}T$ as in Craig, 1989, with c_i and s_i representing $\cos\theta_i$ and $\sin\theta_i$ respectively. Writing ${}^{i-1}_{i}T$ for each joint i and link $i-1$ using the information in each row of Table 1 and

Table 1. The Denavit-Hartenberg Parameters.

joint i, body $(i-1)$	α_{i-1}	a_{i-1}	d_i	θ_i
$i=1$	180°	0	0	θ_1
$i=2$	90°	0	0	θ_2
$i=3$	−90°	0	d_3	θ_3
$i=4$	90°	0	0	θ_4
$i=5$	−90°	0	0	θ_5

multiplying together yields eqns. (1) and (2). Given θ_1-θ_5, homogeneous transformations (1) and (2) may be computed then multiplied to yield ${}^{0}_{5}T = {}^{0}_{3}T\ {}^{3}_{5}T$. The first column of ${}^{0}_{5}T$ is the homogeneous direction ${}^{0}\hat{X}_5$, the pointing direction of the humanoid humerus. Our interest is in the inverse pointing problem where the humerus pointing direction is given and the joint angles must be determined. The serial humanoid shoulder complex in Fig. 2 is kinematically redundant for the purpose of pointing the humeral link ($\hat{X}_5$). It contains five rotations and pointing is a two degree-of-freedom (dof) task. The system has three redundant dof. To resolve two of the redundant dof the condition of humanoid humeral pointing defined in section 2.0 is applied. The $\hat{X}_5$, $\hat{Z}_3$, and $\hat{X}_0$ axes remain coplanar for pointing motions of the humeral link, defining *the humeral plane* shown in a direct and lateral view in left and right sides of Fig. 4. This constraint provides that the pointing systems work synergistically.

$$ {}^{0}_{3}T = \begin{bmatrix} c_1c_2c_3 - s_1s_3 & -c_1c_2s_3 - s_1c_3 & -c_1s_2 & -d_3c_1s_2 \\ -s_1c_2c_3 - c_1s_3 & s_1c_2s_3 - c_1c_3 & s_1s_2 & d_3s_1s_2 \\ -s_2c_3 & s_2s_3 & -c_2 & -d_3c_2 \\ 0 & 0 & 0 & 1 \end{bmatrix} \qquad (1) $$

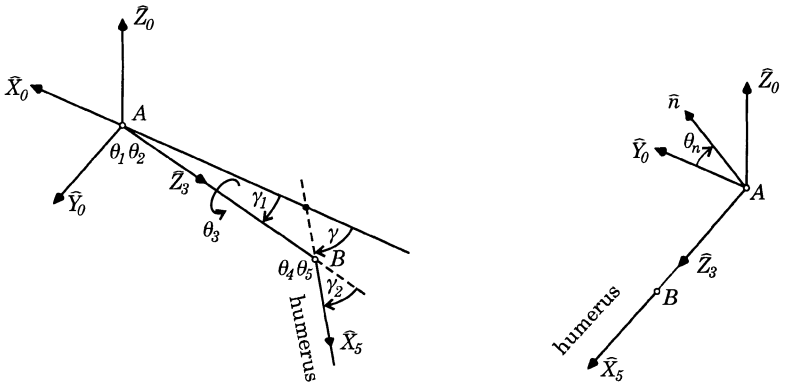

Figure 4. Direct and Lateral views of the humeral plane.

$$ {}^3_5T = \begin{bmatrix} c_4c_5 & -c_4s_5 & -s_4 & 0 \\ s_5 & c_5 & 0 & 0 \\ s_4c_5 & -s_4s_5 & c_4 & 0 \\ 0 & 0 & 0 & 1 \end{bmatrix} \tag{2} $$

Within the humeral plane three interrelated *inclination angles*, γ, γ_1 and γ_2 exist. γ represents the inclination of the humerus from the torso, γ_1 represents the inclination within the humanoid shoulder girdle (related to the human scapular inclination from the torso) and γ_2 represents the inclination of the humerus relative to the scapula. Inclination angles γ_1 and γ_2 are coupled by the human shoulder rhythm.

$$ \frac{\gamma_2}{\gamma_1} = r \quad . \tag{3} $$

where r is approximately 2 for most individuals Let ${}^0\hat{X}_5$, have known desired components x_5, y_5 and z_5,

$$ {}^0\hat{X}_5 = \begin{bmatrix} x_5 \\ y_5 \\ z_5 \end{bmatrix} \tag{4} $$

then the normal to the humeral plane, $\bar{n}$, is found from the vector product,

$$ {}^0\bar{n} = \frac{{}^0\hat{X}_5 \times (-{}^0\hat{X}_0)}{|{}^0\hat{X}_5 \times (-{}^0\hat{X}_0)|} = \begin{bmatrix} 0 \\ -z_5 \\ y_5 \end{bmatrix} \frac{1}{\sqrt{y_5^2 + z_5^2}} \tag{5} $$

and the inclination of the humerus from the torso is found from the scalar product,

$$ \gamma = \cos^{-1}[{}^0\hat{X}_5 \cdot (-{}^0\hat{X}_0)] = \cos^{-1}[-x_5] \quad . \tag{6} $$

Knowing γ from eqn. (6), γ_1 and γ_2 are found by solving eqn. (3) and knowing that γ_1 and γ_2 sum to equal γ (see Fig. 4). Thus,

$$\gamma_1 = \frac{\gamma}{r+1} \ , \tag{7}$$

then γ_2 comes from eqn. (3). Knowing inclination angles γ and γ_1 from eqns. (6) and (7) and the normal direction of the humeral plane from eqn. (5), the direction of the ${}^0\hat{Z}_3$ axis (with components x_3 y_3 and z_3), may be computed. With reference to Figs. 4,

$${}^0\hat{Z}_3 = \begin{bmatrix} x_3 \\ y_3 \\ z_3 \end{bmatrix} \begin{bmatrix} -\cos\gamma_1 \\ \sin\gamma_1 \sin\theta_n \\ -\sin\gamma_1 \cos\theta_n \end{bmatrix} \tag{8}$$

where, $$\theta_n = \text{Atan2}(y_5, -z_5) \tag{9}$$

With ${}^0\hat{Z}_3$ defined above, the solutions for θ_1 and θ_2 come from equating eqn. (8) to the third column of eqn. (1),

$$\theta_2 = \cos^{-1}[-z_3] \tag{10}$$

and, $$\theta_1 = \text{Atan2}(s_1, c_1) = \text{Atan2}\left(\frac{y_3}{s_2}, -\frac{x_3}{s_2}\right) \tag{11}$$

θ_3 effects the values of θ_4 and θ_5. Determination of θ_3 considers performance of a parallel mechanism used to actuate the pointing system centered at A. Suppose θ_3 is known from this consideration. The direction cosine matrix ${}^0_3R$, (the upper left (3×3) portion of ${}^0_3T$ in eqn. 1) can be computed. Then,

$${}^3\hat{X}_5 = {}^0_3R^T \ {}^0\hat{X}_5 \tag{12}$$

which when equated to ${}^3\hat{X}_5$ in eqn. (2) (the first column of ${}^3_5R$) can be solved for θ_4 and θ_5,

$$\theta_5 = \sin^{-1}[-x_5(c_1c_2s_3 + s_1c_3) + y_5(s_1c_2s_3 - c_1c_3) + z_5s_2s_3] \tag{13}$$

$$\theta_4 = \text{Atan2}(s_4, c_4) \tag{14}$$

where, $$s_4 = \frac{-x_5c_1s_2 + y_5s_1s_2 - z_5c_2}{c_5}$$

and, $$c_4 = \frac{x_5(c_1c_2c_3 - s_1s_3) - y_5(s_1c_2c_3 + c_1s_3) - z_5s_2c_3}{c_5} \ ,$$

completing the inverse kinematics.

4. The parallel mechanism humanoid shoulder girdle kinematics

Center A of the girdle is shrouded by three extensible legs, l_1, l_2 and l_3 shown in Fig. 3, creating a parallel mechanism for the humanoid shoulder girdle (analogous to the closed-loop human shoulder girdle). The l_i $(i = 1, 2, 3)$ correspond to the values of θ_i $(i = 1, 2, 3)$ which come from the inverse kinematics of the serial humanoid shoulder girdle already determined and are found by computing the distances from the fixed centers f_i to their corresponding moving centers m_i, shown in Fig. 3.

Centers of the spherical joints are arranged on the fixed and moving platforms on circles with uniform 120° spacing as shown in Fig. 3. The radius of the circle of centers on the fixed and moving platform is r_f and r_m respectively, reported in Lenarčič et al.(a), 2000, Lenarčič et al.(b), 2000. Positions of the fixed centers f_i in frame $\{0\}$ are (l_0 is assumed known),

$$ {}^0\bar{r}_{f_1} = \begin{bmatrix} l_0 \\ r_f \\ 0 \end{bmatrix}, \; {}^0\bar{r}_{f_2} = \begin{bmatrix} l_0 \\ -\frac{1}{2}r_f \\ \frac{\sqrt{3}}{2}r_f \end{bmatrix}, \; {}^0\bar{r}_{f_3} = \begin{bmatrix} l_0 \\ -\frac{1}{2}r_f \\ -\frac{\sqrt{3}}{2}r_f \end{bmatrix} \tag{15} $$

and positions of the moving centers m_i in frame $\{3\}$ are,

$$ {}^3\bar{r}_{m_1} = \begin{bmatrix} 0 \\ -r_m \\ 0 \end{bmatrix}, \; {}^3\bar{r}_{m_2} = \begin{bmatrix} -\frac{\sqrt{3}}{2}r_m \\ \frac{1}{2}r_m \\ 0 \end{bmatrix}, \; {}^3\bar{r}_{m_3} = \begin{bmatrix} \frac{\sqrt{3}}{2}r_m \\ \frac{1}{2}r_m \\ 0 \end{bmatrix} \tag{16} $$

The ${}^3\bar{r}_{m_i}$ must be transformed into frame $\{0\}$,

$$ \begin{bmatrix} {}^0\bar{r}_{m_i} \\ 1 \end{bmatrix} = {}^0_3T \begin{bmatrix} {}^3\bar{r}_{m_i} \\ 1 \end{bmatrix} \qquad (i = 1, 2, 3) \tag{17} $$

where ${}^0_3T$ is known from eqn. (1), (θ_1, θ_2 and θ_3 known). Defining ${}^0\bar{l}_i$ as a vector along the extension of leg i $(i = 1, 2, 3)$,

$$ {}^0\bar{l}_i = {}^0\bar{r}_{m_i} - {}^0\bar{r}_{f_i} \tag{18} $$

then the leg lengths are computed from eqns. , (15)-(18) and (1) by,

$$ l_i = |{}^0\bar{l}_i| \quad . \tag{19} $$

which result in the desired values of θ_1, θ_2 and θ_3 satisfying the humeral plane condition.

Finally, the redundancy θ_3 can be resolved by enhancing performance of the humanoid shoulder girdle and/or glenohumeral joint such as,

1 avoiding kinematic singularities of the shoulder girdle,

2 avoiding kinematic singularities of the glenohumeral joint,

3 maximizing overlap within the prismatic pairs of the extensible legs in the shoulder girdle (i.e. maximizing joint stability), or

4 avoiding mechanical interference between the legs of the shoulder girdle.

Control of θ_3 is a balance between these goals. Optimization of one goal does not lead to optimization of another.

5. A passive prototype using elastic elements

The geometric constraint of the humeral plane was implemented into a back-driven model of the shoulder complex. Elastic members attached to the legs of the shoulder girdle and between the moving platform of the shoulder girdle and the humerus constrain the system. The stiffness of the elastic members was "tuned" so that when back-driven, the model would approximate humanoid humeral pointing kinematics. A search was used to tune these stiffnesses as follows. Given a humeral pointing direction the five joint angles which satisfy the condition of humanoid humeral pointing were found by the inverse kinematic equations in section 3.0. The ability to match this optimal performance with the elastically constrained model was measured by the sum of the squared errors, SSE, of the joint angles in the model as described in Eqn. (20).

$$SSE = (\theta_{10} - \theta_1)^2 + (\theta_{20} - \theta_2)^2 + (\theta_{40} - \theta_4)^2 + (\theta_{50} - \theta_5)^2 \qquad (20)$$

where the θ_{i0} $(i = 1, 2, 4, 5)$ are joint angles as computed in section 3.0 and the θ_i are the joint angles that result in prototype with the elastic members. The θ_i minimize the potential energy within the elastic members for a given humeral pointing direction. Varying the ratio of the stiffness of the three inner elastic members to the stiffness of the three outer elastic members, R_s, and varying the connection points of the outer elastic members, a sufficiently small value of SSE was found for a wide range of pointing directions. Over a wide range of humerus pointing directions a suitable value of R_s was found to be approximately 3.0, with a maximum SSE of 0.0062 radians^2.

6. Conclusions

This paper presented the direct and the inverse humanoid humeral pointing kinematics of a humanoid robotic shoulder complex. The design of a passive back-driven prototype incorporating elastic members was reported.

References

Tsuji. T., Morasso, P. G., Goto, K., and Ito K. (1995), Human hand impedance characteristics during maintained posture, *Biol. Cybern.*, pp. 475–485.

Lenarčič, J. (1999), Basic kinematic characteristics of humanoid manipulators, *Laboratory Robotics and Automation*, vol. 11, pp. 31–38.

Lenarčič, J., and Umek, A. (1994), Simple model of human arm reachable workspace, *IEEE Trans. on Systems, Man and Cybern.*, vol. 6, no. 4, pp. 1239–1246.

Zatsiorky, V., *Kinematics of Human Motion*, Human Kinetics Pub.

Kohne, A., Klopčar, N., and Lenarčič, J., A robotic model of the shoulder girdle contraction, *Proc. of ERK'01 Electrotecnical and Computer Science Conf. - Part B*, Portorož, Slovenia, pp. 219–222.

Dvir, Z., and Berme, N. The shoulder complex in elevation of the arm: A mechanism approach, *Journal of Biomechanics*, vol. 11, pp. 219–225.

Inman, V. T., Saunders, J. B., and Abbott, L. C., Observation on the function of the shoulder joint, *Journal of Bone and Joint Surgery*, vol. 26, pp. 1–30.

Umek-Venturini, A., and Lenarčič, J., The kinematics of the human arm elevation in the frontal plane, *Proc. of the 11th Int. Symp. on Biomedical Engineering*, Zagreb, Croatia, pp. 105–108.

Lenarčič, J., Stanišić, M. M., and Parenti-Castelli, V.,(a), Kinematic design of a humanoid robotic shoulder complex, *IEEE Intl. Conf. on Robotics and Automation*, San Fransisco, pp. 27-32.

Lenarčič, J., Stanišić, M. M., and Parenti-Castelli, V.,(b), A 4 dof parallel mechanism simulating the movement of the human sternum-clavicle-scapula complex, *Advances in Robot Kinematics*, eds. J. Lenarčic and M.M. Stanišić, pp. 325–333.

Craig, J. J., *Introduction to Robotics: Mechanics and Control*, Addison-Wesley Publishing Co.,